Effect of electron injection on defect reactions in irradiated silicon containing boron, carbon, and oxygen

L. F. Makarenko,[1,a)] S. B. Lastovskii,[2] H. S. Yakushevich,[2] M. Moll,[3] and I. Pintilie[4]
[1]*Belarusian State University, Independence Ave. 4, Minsk 220030, Belarus*
[2]*Scientific-Practical Materials Research Centre of NAS of Belarus, Minsk, Belarus*
[3]*CERN, European Organization for Nuclear Research, Geneva, Switzerland*
[4]*National Institute of Materials Physics, Atomistilor 105 bis, Magurele 077125, Romania*

(Received 28 October 2017; accepted 4 January 2018; published online 25 January 2018)

Comparative studies employing Deep Level Transient Spectroscopy and C-V measurements have been performed on recombination-enhanced reactions between defects of interstitial type in boron doped silicon diodes irradiated with alpha-particles. It has been shown that self-interstitial related defects which are immobile even at room temperatures can be activated by very low forward currents at liquid nitrogen temperatures. Their activation is accompanied by the appearance of interstitial carbon atoms. It has been found that at rather high forward current densities which enhance B_iO_i complex disappearance, a retardation of C_i annealing takes place. Contrary to conventional thermal annealing of the interstitial boron-interstitial oxygen complex, the use of forward current injection helps to recover an essential part of charge carriers removed due to irradiation. *Published by AIP Publishing.*
https://doi.org/10.1063/1.5010965

I. INTRODUCTION

Silicon doped with boron is widely used in semiconductor device manufacturing. For example, most silicon solar cells are produced on p-type silicon.[1] One of the reasons to use p-type silicon is its higher radiation tolerance as compared to n-type silicon (n-Si).[2,3]

High levels of radiation tolerance is also an important feature required for particle detectors used in experiments at the Large Hadron Collider (LHC).[4] While for the presently operated LHC silicon strip tracking detectors predominantly n-type silicon is used, the future High Luminosity LHC microstrip sensors will be made out of p-type silicon to exploit their improved radiation tolerance.[5] Furthermore, new sensor concepts based on p-type silicon are under development for High Energy Physics Experiments, like Low Gain Avalanche Detectors (LGADs) for fast timing[6] or the development of CMOS monolithic sensors.[7] These recent developments and the fact that these new devices have to operate in very harsh radiation fields have triggered high interest in the radiation induced defect kinetics in boron doped silicon.

When irradiated with charged particles, the radiation damage associated with the removal of charge carriers in n-type silicon (n-Si) is mainly due to the formation of vacancy-type defects (divacancy, A and E centers).[8] In p-Si, an important role in the removal of charge carriers is related with interstitial defects. In the case of electron irradiation, self-interstitial silicon atoms (Si_i), produced as the main primary defects, displace atoms of group III dopants from their regular substitutional positions already at temperatures $\leq$20 K.[9,10] But in the case of irradiation with heavy particles, the Si_i reactions with impurity atoms are characterized by rather high time constants even at room temperatures (RTs).[11–13]

The processes of interaction of Si_i with impurities can be accelerated upon excitation of the electron-hole subsystem of the crystal. That is, the effect of radiation on the electrical properties of p-Si will depend not only on the particle type and the radiation dose, but also on the dose rate (i.e., particle flux) and external excitation provided by, e.g., illumination or injection of minority charge carriers. The effect of light injection induced performance degradation after irradiation of silicon solar cells has been reported previously.[14,15] In n-type silicon, injection induced transformations of radiation induced defects by external excitation have been observed in bipolar transistors[16] and particle detectors.[17] However, as has been shown by numerous studies,[16–20] this effect is associated with the bistability of vacancy-type defects. Recombination-accelerated reactions related to irradiation induced vacancies are observed at low temperatures[21,22] and do not have a significant effect on the kinetics of radiation damage at room temperatures.

The appearance of silicon interstitial atoms induced by irradiation initiates a series of branching reactions, which are described in Refs. 10 and 23. As a result of these reactions, interstitial impurity atoms appear in the crystal and their migration can also be substantially accelerated by external excitation. For interstitial boron (B_i) and aluminum (Al_i) atoms, this effect was studied in detail using Electron Paramagnetic Resonance and Deep Level Transient Spectroscopy (DLTS) methods.[24,25] In addition, these studies confirm the efficiency of the DLTS junction-capacitance method to explore recombination-enhanced defect reactions, as it was shown earlier in Refs. 26 and 27.

Compared to B_i and Al_i, the experimental data on recombination enhancement of interstitial carbon (C_i) reactions look ambiguous. Although the enhancement of C_i disappearance under excitation by a beam of low-energy electrons was reported in Ref. 28, no quantitative characteristics of this process could be obtained. Moreover, in Ref. 25, where recombination-enhanced annealing in aluminum-doped crystals was investigated, no effect of external excitation on the annealing rate of C_i was observed.

a)makarenko@bsu.by

The excitation effect complicates the analysis of the formation kinetics for radiation defects in p-Si, and the available experimental data on recombination-enhancement of interstitial defect reactions are insufficient to predict the radiation damage of bipolar transistors or solar cells irradiated at different regimes of their operation.

The aim of this paper is to study characteristic features of forward current enhanced (FCE) annealing of three species of interstitial defects: Si_i, C_i, and B_iO_i, produced in boron-doped silicon crystals by irradiation with α-particles.

II. EXPERIMENTAL

Epitaxial Si n^+-p structures (diodes with crystal size $2.8 \times 3.2\,mm^2$, active area $2.3 \times 2.7\,mm^2$, and junction depth $7.2\,\mu m$) with different boron contents in the base region have been used in our experiments. The hole concentration in these structures was estimated from capacitance-voltage measurements to be about $9 \times 10^{14}\,cm^{-3}$ (set 1), $2 \times 10^{14}\,cm^{-3}$ (set 2), and $5 \times 10^{13}\,cm^{-3}$ (set 3) and is mainly due to the doping with boron during the epitaxial growth of the silicon layers of about $50\,\mu m$ thickness. These diodes were produced by the same technological processes resulting in an oxygen content of about $[O] = 1.5 \times 10^{17}\,cm^{-3}$ as determined from the annealing rate of interstitial carbon by using the calibration procedure presented in Ref. 29. This value is consistent with oxygen solubility in the temperature range used for phosphorous diffusion (1050–1100 °C).[30,31] The carbon concentration was evaluated using the ratio between capture cross sections of self-interstitials by boron and carbon[10] and has a value not higher than $2 \times 10^{15}\,cm^{-3}$ in all of our samples.

Irradiations with alpha-particles from a Pu-239 surface source were performed at about 280–290 K. Its surface activity was about $2 \times 10^8\,Bq/cm^2$. The alpha-particle energies were 5.144 MeV and 5.157 MeV and the irradiation time was between 40 and 450 min. The damage distribution for this kind of irradiation source is described in Ref. 29.

The electrically active defects induced by irradiation with alpha-particles were investigated by means of the DLTS technique in the 79–270 K temperature range. Further on, we will use two notations for the recorded spectra: DLTS, when injection pulses are performed with majority-carriers (0 V or reverse bias filling pulses) and MC-DLTS when also minority carriers are injected during the pulses (forward bias filling pulses).

C-V measurements were performed at room temperature (RT) with reverse bias in the range 0–150 V. The distribution of charge carriers (holes) in the diode base was calculated from C-V characteristics using the finite-difference technique.[32]

Conventional thermal annealing of the diodes above 100 °C was performed in air using a temperature-regulated tube oven. Below 100 °C, the samples were annealed *in situ* in the DLTS apparatus.

III. EXPERIMENTAL RESULTS

A. FCE annealing of silicon self-interstitials

The detection of mobile silicon atoms (Si_i) formed as a result of irradiation is usually deduced from the appearance of interstitial atoms of the present impurities, boron (B_i), aluminium (Al_i), or carbon (C_i). These interstitial impurity atoms are reliably identified by the EPR, Infrared Spectroscopy (IR) absorption, and DLTS methods.[10] In p-type silicon, the DLTS method is able to detect the carbon-related centers C_i ($E(0/+) = E_v + 0.28\,eV$) and C_iO_i ($E(0/+) = E_v + 0.36\,eV$). The MC-DLTS method allows also to register the B_iO_i complex ($E(0/+) = E_c - 0.23\,eV$). DLTS spectra with peaks associated with these defects were reported in our previous studies (see, for example, Ref. 33), where their energy levels and pre-exponential factors for emissions rates were determined.

In the diodes under study, no interstitial carbon related defects have been observed in the DLTS spectra recorded for set 1 diodes, immediately after irradiation with alpha particles (Fig. 1, curve 1). Only the peak H1 associated with the divacancy[34] and a peak H3′, which has a significantly smaller amplitude, are registered. The nature of the H3′ peak is not yet clear.

The MC-DLTS spectra recorded before FCE annealing were obtained with limited amplitude and filling pulse in order to avoid uncontrolled injection-stimulated reactions. Short filling pulses ($t_p = 10^{-5}\,s$) with a small forward voltage ($U_p = +0.66\,V$) were used. In the corresponding MC-DLTS spectrum obtained immediately after irradiation (Fig. 1, curve 1′), we observe an additional peak which was labelled in earlier studies as E039 (Ref. 12) and related with the Si self-interstitials (Si_i).[12,35] The inability to use larger forward voltages for the measurement does not allow to determine the maximal amplitude of the E039 peak, limiting thus the use of the MC-DLTS data for quantitative determination of defect concentration.

The E039 peak disappears after a short-time pulse of direct current with a very low density ($J_f = 0.016\,A/cm^2$) even at liquid nitrogen temperature (LNT). Simultaneously with its disappearance, the H2 peak associated with C_i begins to grow (Fig. 1, curve 2). The steady-state concentration of

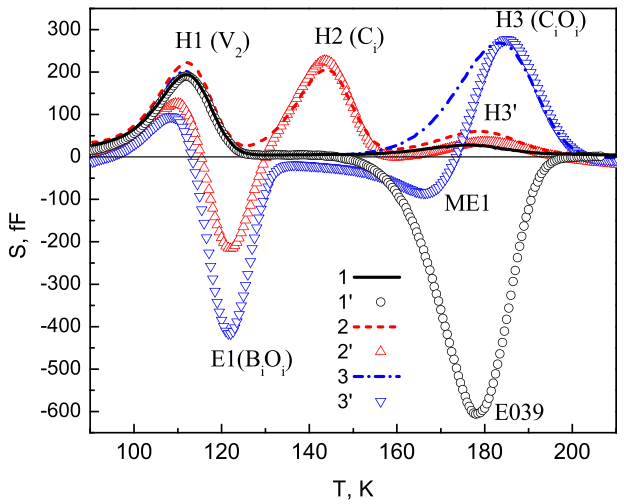

FIG. 1. Conventional DLTS (lines) and MC-DLTS (points) spectra registered immediately after irradiation (1-1′), after FCE annealing at 80 K with forward current density $J = 0.016\,A/cm^2$ during 2 min (2-2′), and after subsequent thermal annealing at 120 °C (3-3′) – for 30 min. Measurement settings were: emission rate window $e_w = 19\,s^{-1}$ for all spectra, bias change –3 → 0 V, and filling pulse duration $t_p = 10\,ms$ for spectra 1, 2, 3; bias change –3 → +0.66 V and filling pulse duration $t_p = 10\,\mu s$ for spectrum 1′ and bias change –3 → +1 V, and filling pulse duration $t_p = 10\,ms$ for spectra 2′, 3′.

C_i is reached after FCE annealing for 30 s. The rate (i.e., the inverse time constant) of the H2 peak formation at $J_f = 0.016$ A/cm^2 is 0.18 s^{-1}. This annealing rate significantly exceeds the analogous value for other interstitial defects (B_i, C_i) in p-Si which under these injection conditions at low temperatures can be considered immobile. Nevertheless, after such a low-temperature injection, another interstitial type defect is observed in the MC-DLTS spectra, namely, B_iO_i (peak E1).[10]

The appearance of this peak is unexpected under the used experimental conditions. Although mobile self-interstitials are captured by C_s and B_s concurrently,[10,23] the formed C_i and B_i complexes are expected to be immobile and thus cannot lead to the formation of C_iO_i or B_iO_i complexes under our experimental conditions. The very small current density used in our FCE annealing is as well not expected to enhance the migration of B_i.

Furthermore, there is no correlation between the growth of the H2 peak (C_i) and the E1 peak (B_iO_i). We have found that while in the course of low-temperature FCE annealing with $J_f = 0.016$ A/cm^2, a gradual increase in the C_i concentration with injection time takes place, the B_iO_i concentration practically does not change. According to previous studies,[36] higher densities of forward current or higher annealing temperatures are needed to grow the E1 peak amplitude.

The growth of the E1 peak amplitude begins in our diodes after thermal annealing at temperatures $\geq$260 K.[36] These temperatures are consistent with the data on B_i annealing in diffused diodes reported in Ref. 24. For annealing temperatures $\geq$280 K, the H2 peak (C_i) disappears and the H3 peak (C_iO_i) concurrently grows (Fig. 1, curves 3 and 3′). After thermal annealing at 120 °C for 30 min, the formation of all radiation-induced interstitial type defects that are stable at room temperature is completed. This thermal treatment will be called in the following the stabilizing anneal.

After the stabilizing anneal, almost all mobile C_i atoms are captured by O_i atoms as evidenced by the changes in the H2 and H3 peaks heights in Fig. 1 and by the results we reported previously.[33] Also, a significant additional formation of the B_iO_i complex takes place (compare the heights of peak E1 in the curves 2′ and 3′ from Fig. 1). In addition to the above-mentioned H1, H3, and E1 peaks, another hole trap (ME1) appears in the MC-DLTS spectra. This peak is associated with a metastable interstitial related defect.[37]

The ratio between the concentrations of radiation-induced interstitial centers containing boron and carbon, manifested in the ratio between the amplitudes of the H3 and E1 peaks after the stabilizing anneal, depends not only on the concentrations of substitutional boron and carbon atoms. As shown in Figs. 2(a) and 2(b), one can observe that the lower the boron content is the smaller the E1 and the larger the H3 peak magnitudes are. However, the amplitudes of E1 and H3 peaks depend also on the post-irradiation treatment. If Si_i (E039) is thermally annealed, then the ratio between the amplitudes of the E1 (B_iO_i) and H1 (V_2) peaks for the diodes of set 1 is $S_{max}(E1)/S_{max}(H1) \cong 7$ [Fig. 2(a), curves 2 and 2′], while if the ratio is calculated from the data after the stabilizing anneal with a preliminary cryogenic FCE

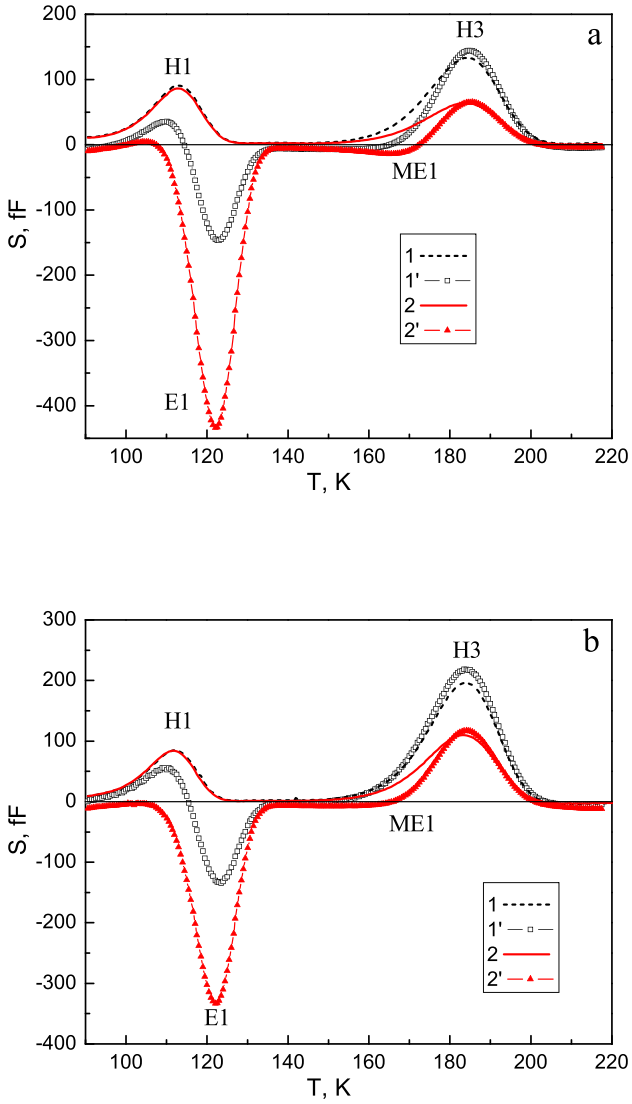

FIG. 2. Comparison of conventional DLTS (1, 2) and MC-DLTS (1′, 2′) spectra for two pairs of diodes with the doping level of $p = 9 \times 10^{14}$ cm^{-3} – set 1 (a) and of $p = 2 \times 10^{14}$ cm^{-3} – set 2 (b). Irradiation of one of the diodes from each pair was followed by current injection at 80 K and subsequent thermal annealing at 120 °C (1, 1′), while the other diode was only thermally annealed without injection at 80 K (2, 2′). Measurement settings were: emission rate window $e_w = 19$ s^{-1} for all spectra, bias change –3 → 0 V, and filling pulse duration $t_p = 10$ ms for spectra 1, 2; bias change –3 → +1 V and filling pulse duration $t_p = 10$ ms for spectra 1′, 2′.

annealing, this ratio becomes much less $S_{max}(E1)/S_{max}(H1) \cong 1.2$ [Fig. 2(a), curves 1 and 1′]. A similar tendency exists for the diodes of set 2 [Fig. 2(b)]. Thus, the injection-stimulated annealing changes not only the rates of interstitial defect reactions, but also the relative probabilities of the interaction between their components. As it has been suggested in Ref. 13, these variations could be a result of the charge state alteration during recombination enhanced diffusion of Si_i.

The injection-induced changes in the formation rates of boron and carbon related defects influence the carrier removal rate in the irradiated diodes. As seen from Fig. 3, the use of FCE annealing helps to reduce the charge-carrier (hole) removal in both sets of diodes. This is expected according to the data presented in Fig. 2, if one takes into

account the number of holes (Δp) removed by irradiation producing B_iO_i and C_iO_i complexes

$$\Delta p = 2N_{B_iO_i} + N_{C_iO_i} f_{C_iO_i}, \quad (1)$$

where $N_{B_iO_i}$ and $N_{C_iO_i}$ are the concentrations of radiation-produced B_iO_i and C_iO_i complexes, and $f_{C_iO_i}$ is an occupancy factor for C_iO_i ($f_{C_iO_i} \leq 1$). The factor 2 in Eq. (1) appears because the formation of each B_iO_i complex accounts for the removal of one B_s acceptor and for one additionally hole trapped from the Si valence band.

It is also necessary to note two important features seen in Fig. 3. The first one is the drop of the boron concentration close to the junction. This drop is due to boron out-diffusion during Si oxidation.[38] Another feature is the registration of damage distribution after irradiation with the surface source of α-particles [Fig. 3(b)]. Such a distribution of the radiation damage was predicted in Ref. 29 and it is related to the irradiation with α-particles, incident at different angles to the diode surface. The maximal depth of radiation damage observed in Fig. 3(b) is consistent with the results of TRIM calculations[39] and can be also considered as a validity test for the performed C-V measurements.

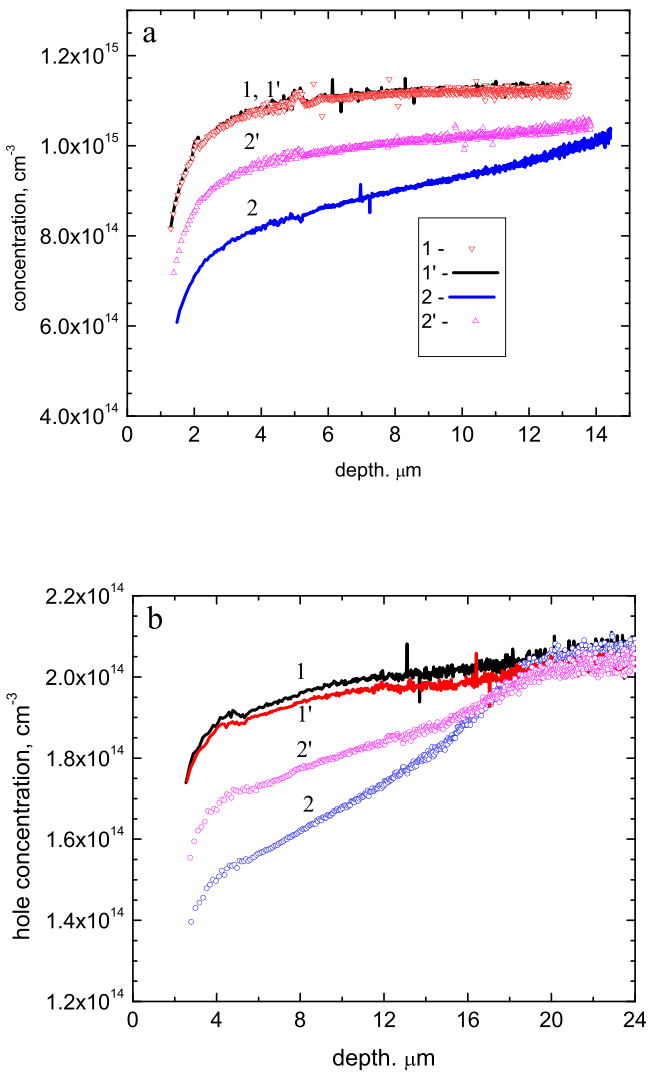

FIG. 3. Changes of the charge carrier (hole) profile (distribution) after different types of post-irradiation treatments for two α-irradiated diodes of set 1 (a) and set 2 (b): 1, 1′ – as-prepared diodes; 2 – after irradiation and stabilizing anneal at 120 °C for 30 min; 2′ – after irradiation, FCE annealing at 78 K with forward current density $J_f = 0.016$ A/cm^2 during 30 min and stabilizing anneal at 120 °C for 30 min.

B. FCE annealing of B_iO_i

The thermal annealing of the B_iO_i complex takes place at the 160–200 °C temperature range.[10,37,40,41] The disappearance of B_iO_i occurs as a result of dissociation and subsequent capture of most of the released B_i atoms by substitutional boron (B_s) generating the B_iB_s complex. Only a very small part of B_i is spent to the formation of B_iC_s complexes in our diodes.[37] Therefore, the reaction of B_i with C_s will be neglected in the following. The thermal annealing rate of B_iO_i slows down with decreasing the boron doping and increasing the oxygen content.[37,40] This is explained by accounting for a partial re-capture of the mobile B_i atoms by interstitial oxygen atoms.[10,37,40]

The B_iB_s complex is neutral[42] and its formation after the annealing of B_iO_i is not expected to lead to a recovery of the free hole concentration because the formation of each neutral B_iB_s center results in removing of two holes from the valence band as previously confirmed experimentally.[41,43]

The results obtained from C-V measurements are consistent with the considered mechanism of B_iO_i annealing. As shown in Fig. 4, only a small increase of the charge carrier concentration takes place after the conventional thermal annealing completely eliminating the B_iO_i complex (curve 3 in Fig. 4).

However, contrary to the conventional thermal annealing, the use of FCE annealing leads to essential growth of the charge carrier concentration (curve 3′ in Fig. 4). This positive effect of FCE annealing can be easily understood by considering that for a recombination enhanced annealing of B_iO_i, no B_iB_s is formed. As the result of the forward current injection, an immediate generation of interstitial carbon atoms takes place.[44] It is clearly seen in Fig. 5 where different MC-DLTS spectra ($\Delta S(T) = S_{Tann}(T) - S_{init}(T)$) are presented. The MC-DLTS spectrum recorded before the FCE annealing is labelled

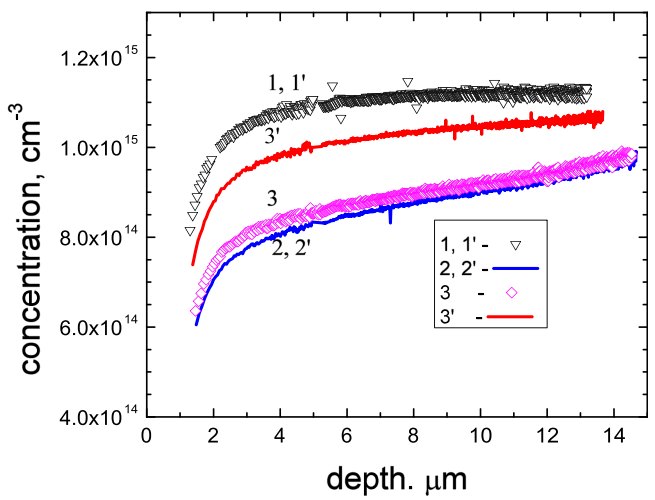

FIG. 4. Changes of the charge carrier (hole) distribution in two identical diodes after complete disappearance of E1-trap (B_iO_i): 1, 1′ – as-prepared; 2, 2′ – after α-irradiation for 450 min and the stabilizing annealing; 3 – after conventional thermal annealing at 200 °C during 60 min; 3′ – after FCE annealing at 320 K during 150 min with forward current density $J_f = 32$ A/cm^2.

as $S_{init}(T)$. The growth of H2 represents the increase of the C_i concentration in the course of annealing. However, for the B_iO_i defect, because the corresponding E1 signal is negative, its height in the difference spectrum represents a decrease in the defect concentration. The twice less height of the H2 peak as compared to that of the E1 peak in Fig. 5 was explained in Ref. 44 as a result of the negative-U properties of the B_iO_i defect. This explanation is also confirmed by the results of theoretical calculations.[45]

Thus, similar to the case of Si_i, the FCE annealing changes not only the rate of annealing-out of the B_iO_i complex, but also it influences the type of defect reaction involved in this process. This fact can be explained as follows. During conventional thermal annealing, all mobile B_i atoms are in the positive charge state and the cross section of their capture by B_s^- is very high due to the Coulomb interaction. Thus, the B_s atoms have a much larger capture radius for the positively charged B_i than for the neutral C_s atoms.[10] On the contrary, during the FCE annealing, the B_i atoms are expected to be in the negatively charged state[24] and the repulsion between B_i^- and B_s^- strongly reduces the probability of forming the B_iB_s complex.

C. Effect of forward current on C_i annealing

The thermal annealing of C_i occurs by its migration until being captured by the interstitial oxygen to form a C_iO_i complex. This process can be studied in detail by monitoring both the initial and final products of the reaction. For example, by employing Infrared Spectroscopy (IR) and DLTS experiments, it has been found that the C_iO_i complex has a series of metastable configurations which are observed during annealing of C_i.[46–48]

The peak position of the metastable state of the C_iO_i complex (C_iO_i*) in DLTS spectra is very close to the position of peak H3′ registered immediately after irradiation (curve 1 in Fig. 1). Thus, for a more precise analysis of C_i annealing, it is preferable to use not the DLTS spectra obtained at different stages of annealing but their differences as it was done for the analysis of B_iO_i annealing. As the reference, we have chosen the spectrum after annealing at $T_{ann} = 270$ K namely $S_{270K}(T)$. Then, in the difference spectrum $\Delta S(T) = S_{Tann}(T) - S_{270K}(T)$, a decrease in the amplitude of the negative signal in the 145 K region corresponds to a decrease in the C_i concentration, and an increase in the amplitude of the positive signal in the 185 K region corresponds to an increase of the C_iO_i concentration (Fig. 6). As can be seen from Fig. 6, in the course of the FCE annealing, a 1:1 ratio between the heights of the H2 and H3 peaks is observed. That is, in the course of both the FCE and conventional thermal annealing, all the available C_i atoms are spent to produce C_iO_i complexes (Fig. 6). However, the formation of the metastable state ($C_iO_i^*$) has not been registered, meaning that the injection of electrons, apparently, influences the $C_iOi^* \rightarrow C_iO_i$ reaction.

The changes in the C_i concentration during isochronal thermal annealing of all types of diodes and the FCE annealing of a diode from set 2 are shown in Fig. 7. The curve for FCE annealing is plotted taking into account the self-heating correction. The coincidence of points 1, 2, and 3 in Fig. 7 obtained using conventional thermal annealing, indicates the same oxygen content in all sets of diodes. This result is expected, since the oxygen penetration into the epitaxial layers has occurred by its diffusion from the oxide during the production of all the investigated diodes.

As seen in Fig. 7, the forward current injection does not cause an enhancement of the C_i annealing, but on the contrary, a retardation of the disappearance rate takes place. However, the activation energy of C_i annealing remains the same as in the case of conventional thermal annealing ($E_{ann} \cong 0.77$ eV).

In our opinion, the retardation of C_i annealing under forward current injection can be related to the smaller

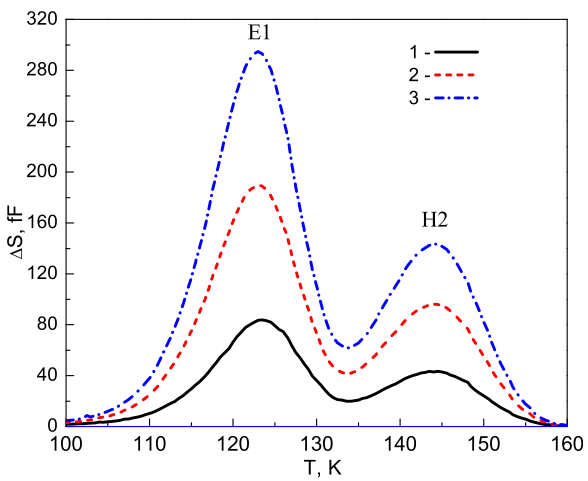

FIG. 5. Difference MC-DLTS ($\Delta S(T) = S_{Tann}(T)$ - $S_{init}(T)$) spectra registered before and in the course of FCE annealing of B_iO_i at 260 K. Curve 1 represents data obtained after 5 min annealing with forward current density $J_f = 24$ A/cm^{-2}, 2 – after subsequent 5 min annealing with $J_f = 32$ A/cm^{-2}, and 3 – after additional 12 min annealing with $J_f = 32$ A/cm^{-2}. The reference spectra ($S_{init}(T)$) were obtained after FCE annealing at 260 K with lower current density (16 A/cm^{-2}). The diode doping level is $p = 2 \times 10^{14}$ cm^{-3} (50 Ω cm).

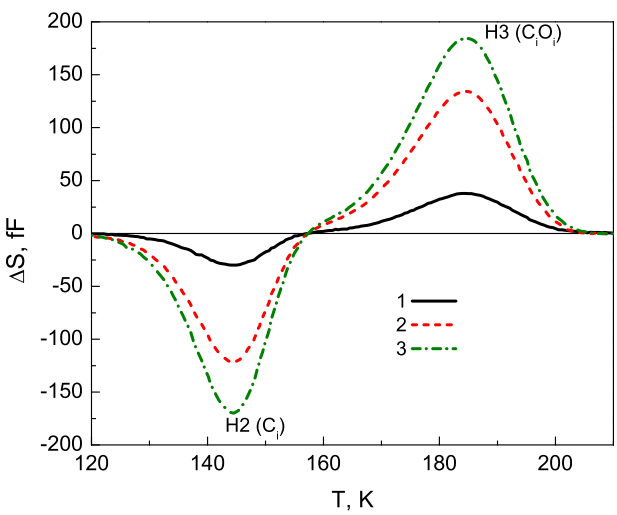

FIG. 6. Difference DLTS ($\Delta S(T) = S_{Tann}(T)$ - $S_{270K}(T)$) spectra registered before and in the course of isochronal FCE annealing of C_i. Doping level of the diode base is $p = 2 \times 10^{14}$ cm^{-3} (50 Ω cm – set 2). Annealing temperatures were: curve 1 – 280 K, curve 2 – 300 K, and curve 3 – 310 K. The annealing time was 15 min with forward current density $J_f = 32$ A/cm^2.

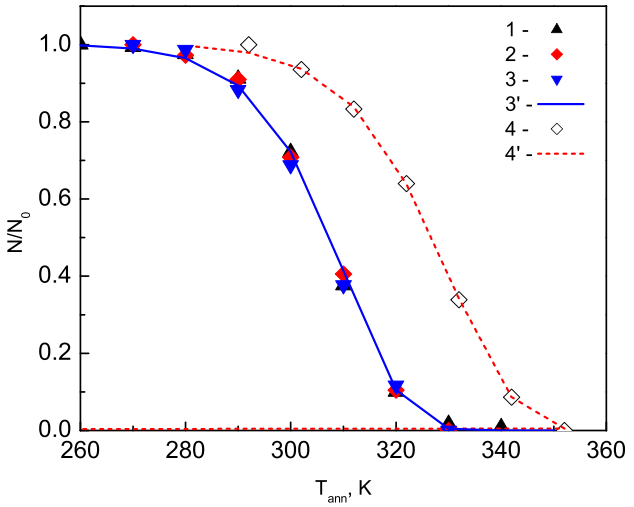

FIG. 7. Isochronal thermal (1, 2, 3) and FCE (4) annealing behaviour of the H2 DLTS-peak (C_i). The scatters represent the experimental data for: 10 Ω cm - set 1 diodes (up triangles), 50 Ω cm set 2 diodes (diamonds), and 250 Ω cm set 3 diodes (down triangles). The annealing time was 15 min with a forward current density $J_f = 32$ A/cm^2. Curves 3′ and 4′ represent the fitting results with an activation energy of 0.77 eV.

probability of forming different metastable states of the close C_i and O_i pairs. However, it seems that in order to get unambiguous evidences for this explanation, a more detailed study of C_i annealing is required.

IV. DISCUSSION

In spite of many research studies, some properties of self-interstitials in silicon still remain under debate. One of the problems is how to explain why in electron-irradiated p-type crystals self-interstitials can migrate at deep cryogenic (<20 K) temperatures[9] but are kept immobile at room temperature under α-irradiation.[12] The main problem here is to determine if self-interstitials are presented as single isolated centers or they are bound ("sticked") to another lattice defect (e.g., an impurity atom). However, the available experimental data does not give a definite solution for this problem. Our experimental data on the process of interstitial defect formation in p-Si crystals under different post-irradiation treatments can be explained by two ways. First, let us accept the suggestion that the E039 trap is related to isolated Si self-interstitial atoms which are immobile at room temperature.[12,35] Then, the appearance of B_iO_i after injection at LNT could be explained considering that a certain fraction of Si_i atoms is formed quite close to the already existing B_sO_i complex, which presumably has a large radius for the capture of silicon self-interstitials. Then, if we suppose the existence of attractive forces between these defects, reaction (2) can take place without involving the B_i migration

$$B_sO_i + Si_i \rightarrow B_iO_i. \quad (2)$$

In the same way, the formation of the H3′ peak can also be explained if one assumes that this peak corresponds to the metastable state of the C_iO_i complex.

Another explanation of B_iO_i detection after low current injection at LNT could be done if one suggests that all self-interstitials are mobile under irradiation at room temperature (RT). Most of their part is trapped by unknown sinks which are kept immobile. A small part of them can be trapped by substitutional boron and carbon and the production of B_i and C_i takes place. Because B_i and C_i can migrate at RT, they are able to form B_iO_i and C_iO_i complexes (and its metastable state $C_iO_i^*$) already during irradiation.

It is important to note that the FCE annealing influences the ratio between the self-interstitials trapped by boron and carbon. This influence can be used to explain the characteristic features of introduction rates of boron and carbon related centers in materials with different doping levels found earlier.[10,41] As was shown in Ref. 41, there is a power-law dependence of the B_iO_i introduction rate with the increasing boron content and the exponent can be essentially less than unity. As a rule, the studies of radiation defects in materials with higher dopant content require higher radiation doses. Accordingly, upon irradiation, particle beams with higher intensities are used. As it was shown above, a larger excitation of the electron-hole subsystem with more intense beams can lead to the suppression of B_iO_i formation while stimulating the generation of C_iO_i. Thus, for interstitial radiation defects, in order to correctly investigate the dependence of their formation rate on the impurity concentration, besides the required information on the impurity content, it is necessary to use also similar irradiation dose rates.

Thus, it is possible that the deviation of the experimental data in Ref. 49 from the conventional point of view regarding the mechanism of B_iO_i formation to be related to a dose rate effect.

As it has been shown in Sec. III B, the use of FCE annealing helps to recover the initial boron concentration. A residual charge carrier removal takes place due to the already existing C_iO_i complexes and additional C_iO_i complexes formed due to the appearance of C_i atoms produced as a result of FCE annealing. That is, the replacement of C_s by B_i takes place. This process is similar to the Watkins replacement mechanism. To explain the replacement of C_s by B_i, we have previously suggested a two-step mechanism.[44] However, it seems a one-step process described in (3) is also possible

$$B_i + C_s \rightarrow B_iC_s^* \rightarrow B_s + C_i. \quad (3)$$

Here, we propose the existence of a specific form of B_iC_s complex which can be produced by forward current injection.

Under conventional thermal annealing, the reaction of carbon replacement proceeds at temperatures ≥300 °C, where the growth in the C_iO_i concentration takes place.[15,41,44] It seems that reaction (3) can also explain an activation stage of implanted boron observed at temperatures 300–400 °C.[50]

V. CONCLUSIONS

The use of α-irradiation made possible to obtain new data on the reactions of interstitial defects in silicon doped with boron. Immediately after α-irradiation, we have found that most of Si self-interstitials are in the immobile form.

Their activation can be stimulated by a very low electron injection even at liquid nitrogen temperatures. Electron injection is shown to suppress the formation of the interstitial boron-oxygen complex. This suppression is detected in materials with various boron contents.

The performed electron injection has stimulated a higher fraction of self-interstitials capable of forming interstitial carbon related defects. However, the injection of electrons does not lead to an enhancement of the interstitial carbon annealing.

The forward current annealing helps to recover the charge carrier concentration after irradiation of boron-doped silicon crystals.

ACKNOWLEDGMENTS

The authors are grateful to Mr. M. S. Rusetski and V. N. Kazuchits for the help in performing C-V measurements.

This work has been carried out in the framework of the RD50 CERN Collaboration.

I. Pintilie acknowledges the funding through the Core Program No. PN16-4801 (National Ministry of Research and Innovation).

[1]A. Goetzberger, C. Hebling, and H. W. Schock, Mater. Sci. Eng., R **40**(1), 1 (2003).
[2]T. Markvart, J. Mater. Sci.: Mater. Electron. **1**, 1 (1990).
[3]M. A. Green, Prog. Photovoltaics **17**, 183 (2009).
[4]G. Lindström, M. Moll, and E. Fretwurst, Nucl. Instrum. Methods Phys. Res., Sect. A **426**, 1 (1999).
[5]M. Moll, *Astroparticle, Particle, Space Physics, Radiation Interaction, Detectors and Medical Physics Applications*, Astroparticle, Particle and Space Physics, Detectors and Medical Physics Applications Vol. 5, in *Proceedings of the 11th Conference*, edited by C. Leroy, P. Rancoita, M. Barone, A. Gaddi, L. Price, and R. Ruchti (World Scientific, 2010), p. 101.
[6]I. Peric, Nucl. Instrum. Methods Phys. Res., Sect. A **582**, 876 (2007).
[7]G. Pellegrini, P. Fernández-Martínez, M. Baselga, C. Fleta, D. Flores, V. Greco, S. Hidalgo, I. Mandić, G. Kramberger, D. Quirion, and M. Ullan, Nucl. Instrum. Methods Phys. Res., Sect. A **765**, 12 (2014).
[8]V. V. Emtsev and T. V. Mashovets, *Impurities and Point Defects in Semiconductors* (Radio Sviaz, Moscow, 1981).
[9]G. D. Watkins, Mater. Sci. Semicond. Process. **3**, 227 (2000).
[10]L. C. Kimerling, M. T. Asom, J. L. Benton, P. J. Drevinsky, and C. E. Caefer, Mater. Sci. Forum **38**, 141 (1989).
[11]M. Asghar, M. Z. Iqbal, and N. Zafar, J. Appl. Phys. **73**, 4240 (1993).
[12]B. N. Mukashev, K. A. Abdullin, and Y. V. Gorelkinskii, Phys. Status Solidi A **168**, 73 (1998).
[13]L. F. Makarenko, M. Moll, J. H. Evans-Freeman, S. B. Lastovski, L. I. Murin, and F. P. Korshunov, Phys. B: Condens. Matter **407**, 3016 (2012).
[14]R. L. Crabb, IEEE Trans. Nucl. Sci. **20**, 243 (1973).
[15]M. Roux, J. Bernard, R. Reulet, and R. L. Crabb, J. Appl. Phys. **56**, 531 (1984).
[16]R. M. Fleming, C. H. Seager, D. V. Lang, E. Bielejec, and J. M. Campbell, Appl. Phys. Lett. **90**, 172105 (2007).
[17]A. Junkes, D. Eckstein, I. Pintilie, L. F. Makarenko, and E. Fretwurst, Nucl. Instrum. Methods Phys. Res., Sect. A **612**, 525 (2010).
[18]R. M. Fleming, C. H. Seager, D. V. Lang, and J. M. Campbell, J. Appl. Phys. **111**, 023715 (2012).
[19]V. P. Markevich, A. R. Peaker, S. B. Lastovskii, L. I. Murin, J. Coutinho, V. J. B. Torres, P. R. Briddon, L. Dobaczewski, E. V. Monakhov, and B. G. Svensson, Phys. Rev. B **80**, 235207 (2009).
[20]R. Radu, I. Pintilie, L. C. Nistor, E. Fretwurst, G. Lindstroem, and L. F. Makarenko, J. Appl. Phys. **117**, 164503 (2015).
[21]B. L. Gregory, J. Appl. Phys. **36**, 3765 (1965).
[22]J. R. Srour, C. J. Marshall, and P. W. Marshall, IEEE Trans. Nucl. Sci. **50**, 653 (2003).
[23]A. N. Larsen and A. Mesli, "Defects in semiconductors," in *Semiconductors and Semimetals*, edited by L. Romano, V. Privitera, and C. Jagadish (Academic Press, 2015), Vol. 91, Chap. 2, p. 47.
[24]J. R. Troxell and G. D. Watkins, Phys. Rev. B **22**, 921 (1980).
[25]J. R. Troxell, A. P. Chatterjee, G. D. Watkins, and L. C. Kimerling, Phys. Rev. B **19**, 5336 (1979).
[26]D. V. Lang and L. C. Kimerling, Phys. Rev. Lett. **33**, 489 (1974).
[27]L. C. Kimerling, Solid-State Electron. **21**, 1391 (1978).
[28]A. R. Frederickson, A. S. Karakashian, P. J. Drevinsky, and C. E. Caefer, J. Appl. Phys. **65**, 3272 (1989).
[29]L. F. Makarenko, M. Moll, F. P. Korshunov, and S. B. Lastovski, J. Appl. Phys. **101**, 113537 (2007).
[30]J. C. Mikkelsen, *Oxygen, Carbon, Hydrogen, and Nitrogen in Crystalline Silicon* (Materials Research Society Symposia Proceedings, 1986), Vol. 59, p. 19.
[31]A. Borghesi, B. Pivac, A. Sassella, and A. Stella, J. Appl. Phys. **77**, 4169 (1995).
[32]P. Blood and J. W. Orton, Rep. Prog. Phys. **41**, 157 (1978).
[33]L. F. Makarenko, F. P. Korshunov, S. B. Lastovskii, L. I. Murin, and M. Moll, Solid State Phenom. **156**, 155 (2010).
[34]L. C. Kimerling, W. M. Gibson, and P. Blood, in *Defects and Radiation Effects in Semiconductors*, Institute of Physics Conference Series, edited by J. H. Albany (IOP, 1978), Vol. 46, p. 273.
[35]K. A. Abdullin, B. N. Mukashev, M. F. Tamendarov, and T. B. Tashenov, Phys. Lett. A **166**, 40 (1992).
[36]L. F. Makarenko, S. B. Lastovskii, H. S. Yakushevich, M. Moll, and I. Pintilie, Proc. Natl. Acad. Sci. Belarus, Phys. Math. Ser. **3**, 108 (2017).
[37]L. F. Makarenko, S. B. Lastovskii, F. P. Korshunov, M. Moll, I. Pintilie, and N. V. Abrosimov, AIP Conf. Proc. **1583**, 123 (2014).
[38]A. S. Grove, O. Leistiko, Jr., and C. T. Sah, J. Appl. Phys. **35**, 2695 (1964).
[39]Calculations have been performed using SRIM 2008 downloaded from srim.org.
[40]O. V. Feklisova, N. A. Yarykin, and J. Weber, Semiconductors **47**, 228 (2013).
[41]P. M. Mooney, L. J. Cheng, M. Süli, J. D. Gerson, and J. W. Corbett, Phys. Rev. B **15**, 3836 (1977).
[42]J. Adey, J. P. Goss, R. Jones, and P. R. Briddon, Phys. B: Condens. Matter **340**, 505 (2003).
[43]H. J. Stein and R. Gereth, J. Appl. Phys. **39**, 2890 (1968).
[44]L. F. Makarenko, S. B. Lastovskii, H. S. Yakushevich, M. Moll, and I. Pintilie, Phys. Status Solidi A **211**, 2558 (2014).
[45]A. Carvalho, R. Jones, M. Sanati, S. K. Estreicher, J. Coutinho, and P. R. Briddon, Phys. Rev. B **73**, 245210 (2006).
[46]L. I. Khirunenko, Y. V. Pomozov, N. A. Tripachko, M. G. Sosnin, A. V. Duvanskii, L. I. Murin, J. L. Lindström, S. B. Lastovskii, L. F. Makarenko, V. P. Markevich, and A. R. Peaker, Solid State Phenom. **108**, 261 (2005).
[47]L. I. Khirunenko, M. G. Sosnin, Y. V. Pomozov, L. I. Murin, V. P. Markevich, A. R. Peaker, L. M. Almeida, J. Coutinho, and V. J. B. Torres, Phys. Rev. B **78**, 155203 (2008).
[48]L. F. Makarenko, F. P. Korshunov, S. B. Lastovskii, L. I. Murin, M. Moll, and I. Pintilie, Semiconductors **48**, 1456 (2014).
[49]L. Vines, E. V. Monakhov, A. Y. Kuznetsov, R. Kozłowski, P. Kaminski, and B. G. Svensson, Phys. Rev. B **78**, 085205 (2008).
[50]A. R. Chelyadinskii and F. F. Komarov, Phys.-Usp. **46**, 789 (2003).